Available online at www.sciencedirect.com
SCIENCE DIRECT®
Bioorganic & Medicinal Chemistry Letters
Bioorganic & Medicinal Chemistry Letters 15 (2005) 3540–3546

P^2–P^3 conformationally constrained ketoamide-based inhibitors of cathepsin K

David G. Barrett,[a,†] Virginia M. Boncek,[b,‡] John G. Catalano,[a] David N. Deaton,[a,*] Anne M. Hassell,[c] Cynthia H. Jurgensen,[b] Stacey T. Long,[d] Robert B. McFadyen,[a] Aaron B. Miller,[c] Larry R. Miller,[b] J. Alan Payne,[b] John A. Ray,[a] Vicente Samano,[a] Lisa M. Shewchuk,[c] Francis X. Tavares,[a] Kevin J. Wells-Knecht,[e,§] Derril H. Willard, Jr.,[f,✠] Lois L. Wright[g] and Hui-Qiang Q. Zhou[a]

[a]*Department of Medicinal Chemistry, GlaxoSmithKline, Research Triangle Park, NC 27709, USA*
[b]*Department of Molecular Pharmacology, GlaxoSmithKline, Research Triangle Park, NC 27709, USA*
[c]*Discovery Research Computational, Analytical, and Structural Sciences, GlaxoSmithKline, Research Triangle Park, NC 27709, USA*
[d]*Department of World Wide Physical Properties, GlaxoSmithKline, Research Triangle Park, NC 27709, USA*
[e]*Department of Research Bioanalysis and Drug Metabolism, GlaxoSmithKline, Research Triangle Park, NC 27709, USA*
[f]*Department of Gene Expression and Protein Purification, GlaxoSmithKline, Research Triangle Park, NC 27709, USA*
[g]*Discovery Research Biology, GlaxoSmithKline, Research Triangle Park, NC 27709, USA*

Received 21 April 2005; revised 16 May 2005; accepted 17 May 2005

Abstract—An orally bioavailable series of ketoamide-based cathepsin K inhibitors with good pharmacokinetic properties has been identified. Starting from a potent inhibitor endowed with poor drug properties, conformational constraint of the P^2-P^3 linker and modifications to $P^{1'}$ elements led to an enhancement in potency, solubility, clearance, and bioavailability. These optimized inhibitors attenuated bone resorption in a rat TPTX hypocalcemic bone resorption model.

With demographic trends toward increases in the elderly population in developed nations and concomitant increases in the number of patients with osteoporosis, the search for therapeutic interventions to minimize fractures has intensified. Complementing agents that induce net bone formation, such as parathyroid hormone (PTH), are anti-resorptive strategies to reduce bone loss and maintain skeletal integrity.[1] Bone resorption results from secretion of acid and enzymes by specialized cells called osteoclasts. The acid dissolves the mineral, hydroxyapatite, while the proteolytic enzymes degrade the protein components of the bone. The major bone-resorbing protease in osteoclasts is the C1A family cysteine protease, cathepsin K.[2] It rapidly hydrolyzes the major component of bone matrix, type I collagen, in complex with glycosaminoglycans.[3] Inhibition of cathepsin K is therefore expected to decrease bone resorption. In fact, small molecule inhibitors of cathepsin K have been shown to inhibit bone resorption in animal models of osteoporosis.[4] Evidence that cathepsin K plays a similar role in humans can be found in a rare autosomal recessive trait known as pycnodysostosis, which is characterized by short stature, abnormal bone and tooth development, increased bone mineral density, and increased bone fragility. Pycnodysostosis results from deactivating mutations in cathepsin K.[5] Thus, cathepsin K inhibitors could be a novel treatment of osteoporosis.

As part of a larger program to develop novel cathepsin K inhibitors, researchers from these laboratories have

Keywords: Cathepsin K; Cysteine protease inhibitors; Ketoamide.
* Corresponding author. Tel.: +1 919 483 6270; fax: +1 919 315 0430; e-mail: david.n.deaton@gsk.com
† Present address: Lilly Forschung GmbH, Essener Str. 93, 22419 Hamburg, Germany.
‡ Present address: 3040 Cornwallis Road, 111 Hermann Building, Research Triangle Park, NC 27709, USA.
§ Present address: Schering-Plough Research Institute, 2015 Galloping Hill, Kenilworth, NJ 07033, USA.
✠ Deceased.

0960-894X/$ - see front matter © 2005 Elsevier Ltd. All rights reserved.
doi:10.1016/j.bmcl.2005.05.062

recently reported the discovery of ketoamide cathepsin K inhibitors **1** (IC_{50} = 0.79 nM) and **2** (IC_{50} = 0.77 nM).[6–8] To optimize these leads further, which suffered from poor aqueous solubility and metabolic instability, a molecular modeling-based strategy was devised to introduce conformational constraints into the P^2–P^3 linker of analog **1**. In addition, $P^{1'}$ moieties with better drug properties, such as the pyrazole group from compound **2**, were introduced to enhance further the drug properties in a constrained inhibitor. With these goals in mind, the synthesis of inhibitors, exemplified by the generic structure **3** was undertaken.

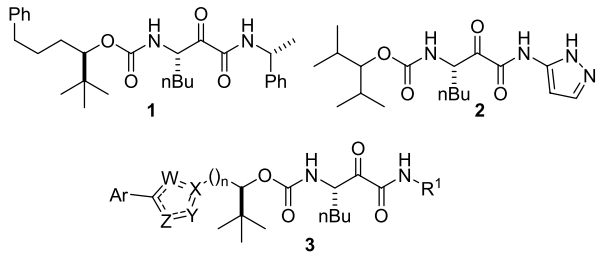

Two general routes were utilized to produce the α-ketoamides. As shown in Scheme 1, one procedure involved joining the chloroformates or *para*-nitrophenylcarbonates, formed from the alcohols **4f–j**, to the β-amino-α-hydroxyamides **5a–e**. The resulting carbamates were subsequently oxidized to the desired ketoamides **6f–k**, **6n**, and **6p–r**.

The other protocol utilized the Wasserman acyl cyanophosphorane oxidative cleavage and amine coupling procedure to generate the ketoamide moiety.[9] As displayed in Scheme 2, alcohols **4a–f** were coupled to a known ester-containing isocyanate **7**.[6] The ester

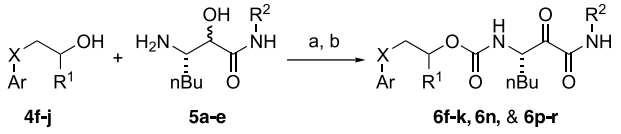

Scheme 1. (a) Reagents and conditions: *para*-Nitrophenyl chloroformate, pyridine, CH_2Cl_2, or 1.93 M $COCl_2$ in PhMe, 46–99%; **5a–e**, *i*-Pr_2NEt, DMF, 54–83%; (b) Dess-Martin periodinane, CH_2Cl_2, 71–83%.

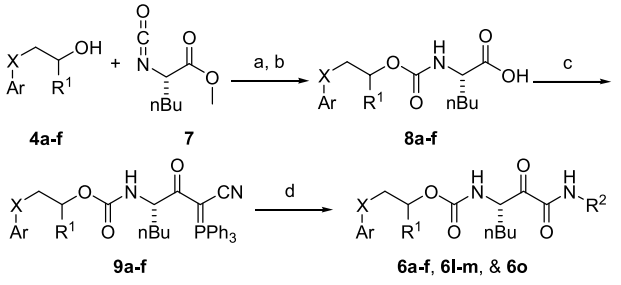

Scheme 2. Reagents and conditions: (a) PhMe, 85 °C, sealed tube, 77–99%; (b) LiOH·H_2O, THF, H_2O; 1 N HCl; (c) Ph_3P=CCN, DMAP, EDC, CH_2Cl_2, 29–76% over two reactions; (d) O_3, CH_2Cl_2, −78 °C; N_2; amine, −78 °C to rt; $AgNO_3$, THF, H_2O, 11–48%.

functional groups of the resulting carbamates were hydrolyzed to yield acids **8a–f**, which were coupled with cyanomethyltriphenylphosphonium ylide to afford the phosphoranes **9a–f**. Then, oxidative cleavage of the phosphorus–carbon double bond with ozone generated an acyl nitrile. In situ displacement of the cyanide by (*R*)-α-methylbenzylamine, 5-amino-1-methylpyrazole, (*S*)-3-amino-2-piperidinone, or 3-amino-2-oxazolidinone afforded the desired ketoamides **6a–f**, **6l–m**, and **6o**.

The alcohols **4a–j** were prepared, as depicted in Schemes 3 and 4. In the first method, 2-methyl-5-aryl-1,3,4-oxadiazoles **10a–c**, available from refluxing the commercially available hydrazides with triethylorthoacetate in xylenes, were deprotonated and then reacted with aldehydes **11a–c** to afford the racemic alcohols, which were then resolved by chiral chromatography (SFC, MeOH in CO_2, Chiralcel AD) to give alcohols **4a–f**.

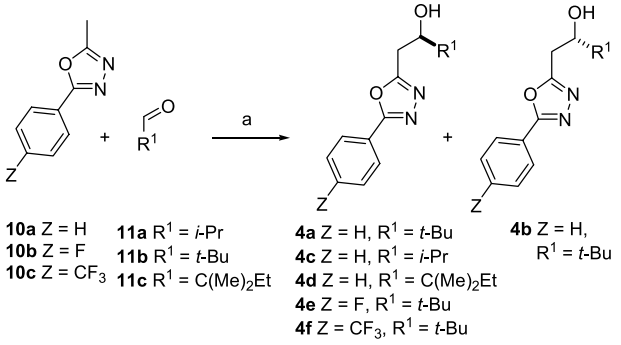

Scheme 3. Reagents and conditions: (a) LiTMP or *n*-BuLi, THF, −78 °C; aldehyde, −78 °C to rt, 11–64%.

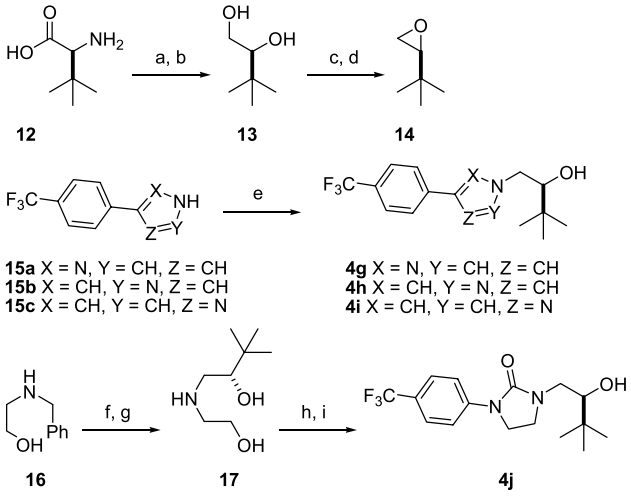

Scheme 4. Reagents and conditions: (a) H_2SO_4, $NaNO_2$, H_2O, 0 °C, 65%; (b) $LiAlH_4$, THF, 0 °C to rt, 63%; (c) TsCl, pyridine, 0 °C to rt, 85%; (d) NaOH, MeOH, H_2O, 0 °C, 83%; (e) **14**, NEt_3, *i*-PrOH, 85 °C, sealed tube, 53–84%; (f) **14**, EtOH, 85 °C, sealed tube, 98%; (g) H_2/Pd-C, MeOH; (h) 4-$CF_3C_6H_4N$=C=O, THF, 47% over 2 steps; (i) DTAD, Ph_3P, THF, 84%.

Alcohols **4g–j** were prepared via opening of the epoxide **14**, as illustrated in Scheme 4. Starting from (*S*)-L-*tert*-leucine **12**, diazotization of the amine and trapping with water provide the α-hydroxyacid, which was subsequently reduced to afford the diol **13**. Then, selective conversion of primary alcohol to tosylate, followed by cyclization with base, gave the epoxide **14**. Heating of pyrazole **15a**, pyrazole **15b**, or imidazole **15c** with the epoxide **14** in a sealed tube yielded the desired alcohols **4g–i**. To synthesize alcohol **4j**, the protected ethanolamine **16** was alkylated with epoxide **14**, and then the benzyl group was removed by hydrogenolysis to give the aminodiol **17**. Selective reaction of the amine **17** with 4-trifluoromethylphenyl isocyanate provided urea. Subsequent cyclization under Mitsunobu conditions afforded the alcohol **4j**.

The heterocycles **15a–c** were prepared, as shown in Scheme 5. Condensation of acetophenone **18** with ethyl formate gave the β-ketoaldehyde, which was treated with hydrazine to afford pyrazole **15a**. Phenylacetic acid **19** was heated with the Vilsmeier reagent to give γ-dimethylamino-2-propenal that was also condensed with hydrazine to provide pyrazole **15b**. Finally, heating α-bromoketone **20** with formamide afforded imidazole **15c**.

Amines **5a–e** were prepared from a known acid **21**, as shown in Scheme 6.[6] First, the acid **21** was activated by ethyl chloroformate, with concomitant protection of the alcohol as ethyl carbonate. Subsequent condensation with amines **22a–e** and cleavage of the ethylcarbonate afforded the α-hydroxyamides. Then, removal of the carbamate gave the desired amines **5a–e**.

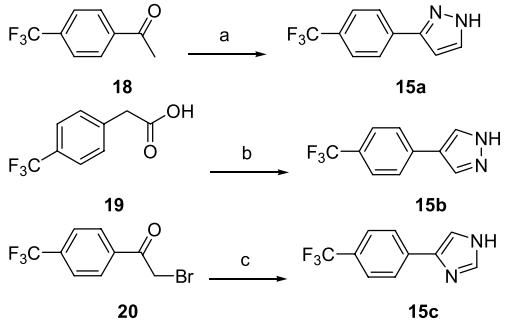

Scheme 5. Reagents and conditions: (a) NaH, EtOCHO, THF, 0 °C to rt; NH_2NH_2, MeOH, 80%; (b) $POCl_3$, DMF, 0 °C to rt; **19**, DMF, rt to 70 °C; K_2CO_3, 0 °C; NaOH, 50 °C; NH_2NH_2, MeOH, 80%; (c) NH_2CHO, 175 °C; 1N HCl, reflux, 67%.

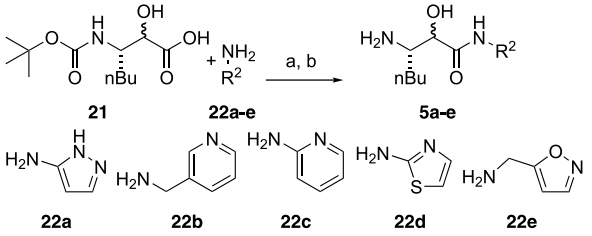

Scheme 6. Reagents and conditions: (a) *N*-methyl piperidine, CH_2Cl_2, −40 °C; EtOCOCl, −40 to 5 °C; **22a–e**, 5 °C to rt; K_2CO_3, H_2O, MeOH, 39–77%; (b) HCl, dioxane, rt.

As shown in Table 1, the oxadiazole constrained ketoamide **6a** is a picomolar inhibitor of cathepsin K (IC_{50} = 0.24 nM) and is 3-fold more potent than inhibitor **1** (IC_{50} = 0.79 nM). Presumably, this slight increase in potency results from a smaller entropic loss due to preconstraining the P^2–P^3 tether, which more than compensates for a higher enthalpic penalty of desolvating an oxadiazole ring as compared to an aliphatic hydrocarbon chain. This desolvation liability is offset by increased hydrophilicity of **6a**, resulting in an increased aqueous solubility (solubility in phosphate buffer at pH 6.8, **6a** = 0.010 mg/mL vs **1** < 0.001 mg/mL). As depicted in Table 2, analog **6a** is moderately selective against cathepsins B (B/K = 50) and L (L/K = 42), with lower selectivity for cathepsins S (S/K = 3) and V (V/K = 7). None of the analogs in Table 2 were potent inhibitors of cathepsin H. This conformational constraint did not enhance the selectivity profile of **6a** versus **1**. Like other ketoamides from these laboratories, the (*S*)-epimer **6b** (IC_{50} = 460 nM) is at least 1000-fold less active than the (*R*)-analog **6a** (**6b** is contaminated with ~0.1% of **6a**).[6,7]

To determine if the *tert*-butyl moiety was still the optimal P^2 substituent in this constrained ketoamide series, the *iso*-propyl analog **6c** and the *tert*-amyl analog **6d** were prepared. Both **6c** (IC_{50} = 0.83 nM) and **6d** (IC_{50} = 1.5 nM) were weaker cathepsin K inhibitors than **6a**. In fact, the bulkier *tert*-amyl derivative **6d** was apparently a more potent cathepsin S inhibitor (IC_{50} = 0.72 nM) than a cathepsin K inhibitor. Given these results, the P^2 group was defined as *tert*-butyl for subsequent SAR development.

Since unsubstituted phenyl groups can be prone to phase I metabolism, fluoro- or trifluoromethyl substituents were introduced into the P^3 phenyl group to sterically and electronically attenuate potential oxidation by Cyp^{450} enzymes. The *para*-fluoro analog **6e** (IC_{50} = 0.37 nM) and the *para*-trifluoromethyl analog **6f** (IC_{50} = 0.41 nM) were equipotent to the parent analog **6a**, and these substituents were incorporated into the further design of inhibitors.

The $P^{1'}$ aryl group in analogs **6a–f** did not aid in aqueous solubility and was also a potential metabolic liability. Building on previous $P^{1'}$ SAR development,[8] the (*R*)-α-phenylethylamine was replaced by the potency- and solubility-enhancing pyrazole, giving inhibitor **6g**. Pyrazole **6g** (IC_{50} = 0.029 nM) was ~10-fold more potent and was slightly more selective than **6f**. Moreover, as shown in Table 3, this pyrazole exhibited excellent permeability in an in vitro Madin–Darby canine kidney (MDCK) permeation assay (P_{APP} = 290 nm/s)[10], as well as improved solubility in fasted state-simulated intestinal fluid (FS-SIF = 0.061 mg/mL)[11,12] at pH 6.8, relative to inhibitor **6a** (FS-SIF = 0.019 mg/mL). With these encouraging predictors of good absorption, the pharmacokinetics of analog **6g** were profiled in male Han Wistar rats. It

Table 1. Inhibition of human cathepsin K

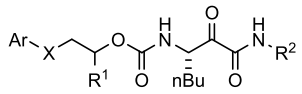

#	Ar	X	R^1	R^2	IC_{50}[a] (nM)
6a		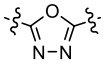			0.24
6b		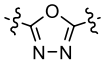			460
6c		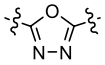			0.83
6d		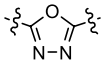			1.5
6e	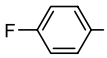	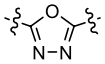			0.37
6f		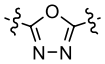			0.41
6g		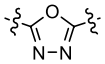			0.029
6h		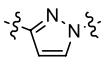			0.072
6i		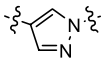			0.032
6j		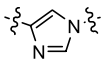			0.026
6k					0.34
6l					4.9
6m					0.65
6n					2.8
6o					0.13
6p					8.1
6q					5.8
6r					0.42

[a] Inhibition of recombinant human cathepsin K activity in a fluorescence assay using 10 μM Cbz-Phe-Arg-AMC as substrate in 100 mM NaOAc, 10 mM DTT, and 120 mM NaCl, pH 5.5. The IC_{50} values are means of two or three inhibition assays, individual data points in each experiment were within a 3-fold range of each other.

Table 2. Cathepsin B, L, S, and V inhibition and selectivity

#	Cat K IC_{50} (nM)	Cat B IC_{50} (nM)[a]	Cat L IC_{50} (nM)[b]	Cat S IC_{50} (nM)[c]	Cat V IC_{50} (nM)[d]
6a	0.24	12	10	0.75	1.6
6c	0.83	31	17	3.7	5.6
6d	1.5	56	17	0.72	2.8
6e	0.37	9.8	33	0.53	34
6f	0.41	32	190	1.6	5.0
6g	0.029	45	69	0.52	1.2
6h	0.072	20	8.7	0.21	0.17
6i	0.032	10	36	0.078	0.43
6j	0.026	27	10	0.16	0.13
6k	0.34	60	37	0.54	1.7
6l	4.9	3500	3800	110	230
6m	0.65	6.2	15	0.81	1.3
6n	2.8	18	130	2.7	14
6o	0.13	5.2	160	1.2	7.1
6p	8.1	107	240	3.7	4.5
6q	5.8	870	1000	19	36
6r	0.42	23	69	0.12	0.89

[a] Inhibition of recombinant human cathepsin B activity in a fluorescence assay using 10 μM Cbz-Phe-Arg-AMC as substrate in 100 mM NaOAc, 10 mM DTT, and 120 mM NaCl, pH 5.5. The IC_{50} values are means of two or three inhibition assays, individual data points in each experiment within a 2-fold range of each other.

[b] Inhibition of recombinant human cathepsin L activity in a fluorescence assay using 5 μM Cbz-Phe-Arg-AMC as substrate in 100 mM NaOAc, 10 mM DTT, and 120 mM NaCl, pH 5.5.

[c] Inhibition of recombinant human cathepsin S activity in a fluorescence assay using 10 μM Cbz-Val-Val-Arg-AMC as substrate in 100 mM NaOAc, 10 mM DTT, and 120 mM NaCl, pH 5.5.

[d] Inhibition of recombinant human cathepsin V activity in a fluorescence assay using 2 μM Cbz-Phe-Arg-AMC as substrate in 100 mM NaOAc, 10 mM DTT, and 120 mM NaCl, pH 5.5.

Table 3. Pharmacokinetics of combination analogs

#	clog *P*	MDCK P_{APP} (nm/s)	Sol. FS-SIF[a] (mg/mL)	$t_{1/2}$[b] (min)	C_l[c] (mL/min/kg)	V_{SS}[d] (mL/kg)	*F*[e] (%)
6g	3.34	290	0.061	530	11	1900	50
6h	5.55	91	0.11	320	9.6	1600	42
6i	5.34	120	0.097	340	9.1	2100	45
6j	5.08	160	0.13	460	15	2400	55
6k	4.80	—	0.043	340	55	5000	27
6l	2.59	350	0.058	150	33	3600	88
6m	3.10	—	0.62	140	35	1400	17
6n	3.53	280	0.49	230	11	1400	46
6o	4.42	15	0.17	410	11	3100	79
6p	5.96	180	0.38	210	41	1800	34
6q	5.33	76	0.048	280	15	1800	43
6r	5.99	180	0.064	400	3.2	1700	40

[a] FS-SIF is the equilibrium solubility in a fasted state-simulated intestinal fluid at pH 6.8. The values are means of two measurements.

[b] $t_{1/2}$ is the i.v. terminal half-life dosed as a solution in male Han Wistar rats. All in vivo pharmacokinetic values are means of two experiments.

[c] C_l is the total clearance.

[d] V_{SS} is the steady-state volume of distribution.

[e] *F* is the oral bioavailability.

exhibited a long terminal half-life ($t_{1/2}$ = 530 min), with a low clearance (C_l = 11 mL/min/kg) and medium volume of distribution (V_{SS} = 1900 mL/kg). In confirmation of the in vitro permeability and solubility measurements, **6g** was orally bioavailable (*F* = 50%).

To investigate this promising series further, the oxadiazole ring constraint was replaced with other five-membered ring heterocycles. The pyrazoles **6h** (IC_{50} = 0.072 nM), and **6i** (IC_{50} = 0.032 nM) and the imidazole **6j** (IC_{50} = 0.026 nM) were essentially equipotent inhibitors of cathepsin K, whereas the cyclic urea **6k** (IC_{50} = 0.34 nM) was less active. As shown in Table 3, the heteroaryl constraints also demonstrated excellent pharmacokinetic properties in rats ($t_{1/2}$ = 320–460 min, C_l = 9.1–15 mL/min/kg, and *F* = 42–55%). In contrast, the cyclic urea **6k** exhibited a clearance (C_l = 55 mL/min/kg), approaching hepatic blood flow for the rat and a lower oral bioavailability (*F* = 27%), suggesting extensive metabolism.

Since replacement of the $P^{1'}$ α-methylbenzyl with pyrazole resulted in enhanced potency and improved drug properties, the effect of other heterocycles at $P^{1'}$ was investigated. As expected based on previous SAR,[8] the *N*-methyl pyrazole **6l** (IC_{50} = 4.9 nM) was less potent, but exhibited a better selectivity profile than **6e**. It was highly orally bioavailable (*F* = 88%), but exhibited a

higher clearance (C_l = 33 mL/min/kg), relative to the parent pyrazole, possibly due to N-demethylation of the pyrazole. This clearance resulted in a diminished terminal half-life ($t_{1/2}$ = 150 min). Replacement of the pyrazole with further heterocycles lacking a hydrogen bond donor resulted in decreased potency. For example, thiazole **6q** (IC_{50} = 5.8 nM) was ~200-fold less potent than pyrazole **6j** and homologated isoxazole **6r** (IC_{50} = 0.42 nM) was ~6-fold less potent than pyrazole **6h**. The pharmacokinetics of these still potent cathepsin K inhibitors were determined in rats. Thiazole **6q** (C_l = 15 mL/min/kg, F = 43%) showed a profile reminiscent of pyrazole **6j**. The clearance of isoxazole **6r** was extremely low (C_l = 3.2 mL/min/kg) and the oral bioavailability (F = 40%) was good.

An X-ray co-crystal structure of ketoamide **2** with cathepsin K showed that the pyrazole NH forms two hydrogen bonds with the protein. One with the indole NH of ^{184}Trp and a second interaction with ^{19}Gln through bridging water molecules.[8] From a modeling point of view, it has been suggested that the 2-piperidone carbonyl of ketoamide **6m** (IC_{50} = 0.65 nM) and the oxazolidinone carbonyl of ketoamide **6o** (IC_{50} = 0.13 nM) could serve as hydrogen bond acceptors in interactions with the ^{184}Trp indole. However, these analogs were less potent than the pyrazole **6g**. Presumably, the proposed hydrogen bond interaction could not compensate for the loss of both the hydrogen bonds of the pyrazole. The clearance of 2-piperidone **6m** (C_l = 35 mL/min/kg) was approximately half of hepatic blood flow in the rat, and its oral bioavailability (F = 17%) was lower than that of pyrazole **6g**. In contrast, oxadiazolidinone **6o** exhibited a low clearance (C_l = 11 mL/min/kg) and an excellent oral bioavailability (F = 79%), despite moderate in vitro permeability (MDCK P_{APP} = 15 nm/s).

In an attempt to improve further the aqueous solubility of the series, the two pyridine derivatives **6n** (IC_{50} = 2.8 nM) and **6p** (IC_{50} = 8.1 nM) were prepared. Both **6n** and **6p** were significantly less potent cathepsin K inhibitors than **6g** or **6h**, respectively, as expected from the loss of a hydrogen bond donor, and were also less selective versus other cathepsins. Furthermore, the improved solubilities did not lead to a better oral exposure for either **6n** (F = 46%) or **6p** (F = 34%).

Analogs **6g**–**j** were tested in an ex vivo human osteoclast resorption assay.[13] Human peripheral blood monocyte cells were placed in media on bone chips and differentiated into osteoclast-like cells with receptor activator of nuclear factor κ B ligand (RANK-L) and macrophage colony stimulating factor (m-CSF). Then, bone resorption was measured by calcium release into media in the presence or absence of a cathepsin K inhibitor. All four compounds inhibited bone resorption at nanomolar concentrations in this assay, with **6h** (IC_{50} = 120 nM) and **6i** (IC_{50} = 190 nM) being more potent than **6g** (IC_{50} = 690 nM) and **6j** (IC_{50} = 570 nM).

Analogs **6g** (rat IC_{50} = 1.8 nM), **6h** (rat IC_{50} = 1.3 nM), **6i** (rat IC_{50} = 2.0 nM), and **6j** (rat IC_{50} = 1.0 nM) are significantly less potent inhibitors of rat cathepsin K than human cathepsin K (18- to 62-fold). These results can be explained by differences in the active site of the rat and human cathepsin K (^{61}Asp → Tyr in S^3 and ^{133}Ala → Ser in S^2).[2] As expected based on rat cathepsin K IC_{50}s, ketoamides **6h**–**j** were significantly less potent in attenuating deoxypyridinoline crosslink release in an ex vivo rat calvarial resorption assay[14,15] (IC_{50} = 2900–6000 nM) than in a human osteoclast resorption assay. Despite this species-specific loss in potency, inhibitors **6h** and **j** were tested in a thyroid–parathyroidectomized hypocalcemic rat assay (TPTX).[16] In this model, removal of the parathyroid gland eliminated parathyroid hormone (PTH) secretion, altering the maintenance of calcium homeostasis via PTH-stimulated bone resorption. Rapid depletion of calcium from serum occurs when dietary calcium supplementation is prevented. Infusion of hPTH (1–34) at 30,000 ng/kg/h then induces a rapid increase in serum calcium levels. As shown in Table 4, oral administration of cathepsin K inhibitors **6h** or **j** dose-dependently attenuated the PTH-stimulated calcium increase in this model by blocking collagen matrix degradation. These results reached statistical significance at a dose of 100 mg/kg p.o. Because cathepsin K inhibitors do not affect resorption lacunae acidification, some calcium is released by hydroxyapatite dissolution before the collagen fibrils are exposed.[17] Osteoblastic MMP-13 and MMP-14 may also partially compensate for any lack of cathepsin K activity in matrix degradation. Despite these counteractions, treatment of the rats with cathepsin K inhibitors clearly inhibited calcium release from bone.

An X-ray co-crystal structure of cathepsin K with inhibitor **6o** was subsequently solved, providing further insight into the binding mode of these constrained ketoamide inhibitors. The active site is shown in Figure 1. These reversible, time-dependent, tight binding inhibitors form a covalent hemithioketal intermediate between the α-keto moiety of the inhibitor and the active site ^{25}Cys of the enzyme. In contrast to aldehyde and ketone inhibitors bound to cathepsin K, the hemithioketal hydroxyl does not occupy the oxyanion hole, rather it is stabilized by hydrogen bonds to the catalytic

Table 4. Rat TPTX hypocalcemic resorption assay

t (h)		Serum calcium					
		Veh.	PTH	6h		6j	
				30[a]	100[a]	30[a]	100[a]
0	Avg.	1.07	1.07	1.05	1.07	1.12	1.14
	SD	0.07	0.06	0.10	0.04	0.08	0.09
2	Avg.	0.98	1.19	1.14	1.10	1.21	1.16
	SD	0.03	0.08	0.13	0.03	0.09	0.06
4	Avg.	0.94	1.41	1.30	1.21[c]	1.42	1.31[b]
	SD	0.06	0.06	0.07	0.02	0.05	0.07
6	Avg.	0.90	1.64	1.57	1.34[c]	1.63	1.51[b]
	SD	0.04	0.04	0.20	0.07	0.04	0.07

[a] Dose, mg/kg.
[b] $p < 0.05$ compared to PTH control.
[c] $p < 0.01$ compared to PTH control.

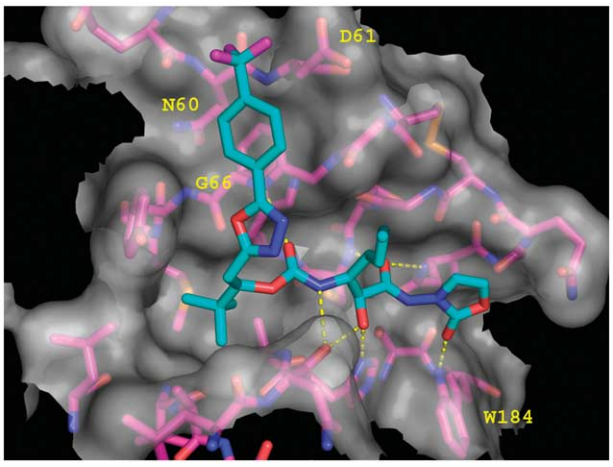

Figure 1. Active site of the X-ray co-crystal structure of compound **6o** complexed with cathepsin K. The cathepsin K carbons are colored magenta, with inhibitor **6o** carbons colored cyan. The semi-transparent white surface represents the molecular surface, while hydrogen bonds are depicted as yellow dashed lines. The coordinates have been deposited in the Brookhaven Protein Data Bank, Accession No. 1YT7. This figure was generated using PYMOL version 0.97 (Delano Scientific, www.pymol.org).

histidine (^{162}His) and the backbone carbonyl of ^{161}Asn, consistent with other ketoamide co-crystal structures of this group.[8,18] The oxyanion hole is occupied by the carbonyl of the amide, which is stabilized by hydrogen bonds to the side chain NH of ^{19}Gln and the backbone NH of ^{25}Cys. The peptide backbone recognition site of the enzyme stabilizes the inhibitor with two additional hydrogen bonds between ^{161}Asn and the carbamate NH and ^{66}Gly and the carbamate carbonyl oxygen.

Apart from these hydrogen bond stabilizing interactions with the protein, the $P^{1'}$ oxazolidinone carbonyl oxygen forms a hydrogen bond with the indole NH of ^{184}Trp, as predicted by modeling. Moreover, the norleucine-derived P^1 group of the inhibitor lies along the S^1 wall formed from ^{23}Gly, ^{24}Ser, ^{64}Gly, and ^{65}Gly, with one face of the *n*-butyl group forming van der Waals interactions with the protease, while its terminal carbon remains solvent exposed. Furthermore, the P^2 *tert*-butyl substituent forms significant lipophilic interactions with the deep S^2 pocket composed of ^{67}Tyr, ^{68}Met, ^{134}Ala, ^{163}Ala, and ^{209}Leu. Finally, the P^3 *para*-trifluoromethylphenyloxadiazole moiety interacts with the active site trough, as well as pointing into the S^3 subsite formed by ^{60}Asn, ^{61}Asp, ^{65}Gly, ^{66}Gly, and ^{67}Tyr.

In summary, this report details the optimization of ketoamide **1** to potent, orally bioavailable cathepsin K inhibitors, such as **6h** and **j**. Conformational constraint was utilized to reduce entropic losses upon inhibitor binding. These efforts led to increased cathepsin K inhibitory activity. Furthermore, the heterocyclic nature of the constraints led to a reduction in hydrophobicity and an improvement in aqueous solubility. Combining these P^2–P^3 changes with more drug-like $P^{1'}$ moieties afforded potent, orally bioavailable cathepsin K inhibitors with good pharmacokinetics in rats. These picomolar inhibitors of human cathepsin K attenuate bone resorption in ex vivo and in vivo animal models of bone resorption. Additional efforts to improve the selectivity of these inhibitors versus other cathepsin endoproteases are warranted.

Acknowledgments

The authors wish to thank Melissa A. Gomez and Manon S. Villeneuve for chiral separations of alcohols **4a**–**f**.

References and notes

1. Einhorn, T. A. In *Osteoporosis*; Marcus, R., Feldman, D., Kelsey, J., Eds.; Academic Press: San Diego, California, 1996, p 3.
2. Deaton, D. N.; Kumar, S. *Prog. Med. Chem.* **2004**, *42*, 245.
3. Li, Z.; Hou, W.-S.; Escalante-Torres, C. R.; Gelb, B. D.; Bromme, D. *J. Biol. Chem.* **2002**, *277*, 28669.
4. Stroup, G. B.; Lark, M. W.; Veber, D. F.; Bhattacharyya, A.; Blake, S.; Dare, L. C.; Erhard, K. F.; Hoffman, S. J.; James, I. E.; Marquis, R. W.; Ru, Y.; Vasko-Moser, J. A.; Smith, B. R.; Tomaszek, T.; Gowen, M. *J. Bone Miner. Res.* **2001**, *16*, 1739.
5. Gelb, B. D.; Shi, G.-P.; Chapman, H. A.; Desnick, R. J. *Science* **1996**, *273*, 1236.
6. Catalano, J. G.; Deaton, D. N.; Long, S. T.; McFadyen, R. B.; Miller, L. R.; Payne, J. A.; Wells-Knecht, K. J.; Wright, L. L. *Bioorg. Med. Chem. Lett.* **2004**, *14*, 719.
7. Barrett, D. G.; Catalano, J. G.; Deaton, D. N.; Long, S. T.; Miller, L. R.; Tavares, F. X.; Wells-Knecht, K. J.; Wright, L. L.; Zhou, H.-Q. Q. *Bioorg. Med. Chem. Lett.* **2004**, *14*, 2543.
8. Tavares, F. X.; Boncek, V.; Deaton, D. N.; Hassell, A. M.; Long, S. T.; Miller, A. B.; Payne, A. A.; Miller, L. R.; Shewchuk, L. M.; Wells-Knecht, K.; Willard, D. H., Jr.; Wright, L. L.; Zhou, H.-Q. *J. Med. Chem.* **2004**, *47*, 588.
9. Wasserman, H. H.; Petersen, A. K. *Tetrahedron Lett.* **1997**, *38*, 953.
10. Irvine, J. D.; Takahashi, L.; Lockhart, K.; Cheong, J.; Tolan, J. W.; Selick, H. E.; Grove, J. R. *J. Pharm. Sci.* **1999**, *88*, 28.
11. Dressman, J. B.; Amidon, G. L.; Reppas, C.; Shah, V. P. *Pharm. Res.* **1998**, *15*, 11.
12. Kostewicz, E. S.; Brauns, U.; Becker, R.; Dressman, J. B. *Pharm. Res.* **2002**, *19*, 345.
13. Nicholson, G. C.; Malakellis, M.; Collier, F. M.; Cameron, P. U.; Holloway, W. R.; Gough, T. J.; Gregorio-King, C.; Kirkland, M. A.; Myers, D. E. *Clin. Sci.* **2000**, *99*, 133.
14. Hahn, T. J.; Westbrook, S. L.; Halstead, L. R. *Endocrinology* **1984**, *114*, 1864.
15. Conaway, H. H.; Grigorie, D.; Lerner, U. H. *J. Endocrinol.* **1997**, *155*, 513.
16. Thompson, D. D.; Seedor, J. G.; Fisher, J. E.; Rosenblatt, M.; Rodan, G. A. *Proc. Natl. Acad. Sci. U.S.A.* **1988**, *85*, 5673.
17. Kiviranta, R.; Morko, J.; Alatalo, S. L.; NicAmhlaoibh, R.; Risteli, J.; Laitala-Leinonen, T.; Vuorio, E. *Bone* **2005**, *36*, 159.
18. Barrett, D. G.; Catalano, J. G.; Deaton, D. N.; Hassell, A. M.; Long, S. T.; Miller, A. B.; Miller, L. R.; Shewchuk, L. M.; Wells-Knecht, K. J.; Willard, D. H., Jr.; Wright, L. L. *Bioorg. Med. Chem. Lett.* **2004**, *14*, 4897.